

## SEARCH FOR SOFT GAMMA REPEATERS IN THE SMM/HXRBS DATA

C. KOUVELIOTOU,<sup>1,2,3</sup> J. P. NORRIS,<sup>4</sup> K. S. WOOD,<sup>5</sup> T. L. CLINE,<sup>6</sup> B. R. DENNIS,<sup>7</sup>  
 U. D. DESAI,<sup>7</sup> AND L. E. ORWIG<sup>7</sup>

Received 1989 September 15; accepted 1991 December 16

### ABSTRACT

Bursts from the soft gamma-ray repeaters (SGRs) appear to constitute a class of high-energy transients separate from typical gamma-ray bursts. Their distinct characteristics include stochastic burst repetition, short ( $\sim 0.1$  s) durations, simple time histories, rise times as fast as 5 ms, spectra with characteristic energies of  $\sim 30$  keV, and no indication of spectral evolution on time scales as short as  $\sim 0.1$  s. Presently, only three repeaters are known. Thus, fundamental questions regarding their typical active lifetimes, celestial distribution, and luminosity function remain unresolved.

We describe the results of a search for short transients resembling SGR bursts using the triggered fast memory of the hard X-ray burst spectrometer (HXRBS) on board the *Solar Maximum Mission* (SMM). This instrument operated for almost 10 years, from its launch in 1980 February until its demise in 1989 December. Each year its  $40^\circ$  FWHM field of view scanned approximately one-quarter of the sky in the form of a band about  $80^\circ$  wide centered on the ecliptic. HXRBS had a unique triggering capability with very short integration times of 4, 32, and 256 ms that made it ideal for detecting short, intense events. The effective HXRBS sensitivity for detecting SGR-like bursts longer than  $\sim 20$  ms was routinely  $\sim 4 \times 10^{-7}$  ergs  $\text{cm}^{-2}$ , and occasionally  $8 \times 10^{-8}$  ergs  $\text{cm}^{-2}$ .

This search adds to the coverage by the *International Cometary Explorer* (ICE) of the most active repeater, SGR 1806–20, and indicates that the highly active phase of this source has not continued beyond 1984. We have found no other SGR-like source, but we identify some candidate events. Our results, combined with results from ICE and Konus observations and the assumption of a neutron star origin, enable us to make estimates of the burst-active time of an SGR source. In addition, we calculate the noise environment of the HXRBS CsI(Na) crystal on board SMM, a spacecraft in a low-inclination/low-altitude orbit, to be  $1.5 \times 10^{-4}$  events  $\text{s}^{-1}$ .

*Subject headings:* gamma rays: bursts — gamma rays: observations

### 1. INTRODUCTION

From the few hundred gamma-ray bursters (GRBs) known today, only three have been observed to repeat. They now fall into a distinct class of high-energy transients known as the soft gamma-ray repeaters (SGRs). The first two SGRs were discovered in 1979 in the data of the Konus experiment aboard the *Venera 11–14* spacecraft (Golenetskii, Il'inskii, & Mazets 1984; Mazets, Golenetskii, & Gur'yan 1979). The third SGR was discovered shortly after the community was alerted by Hurley (1986), who suggested that several events detected with *Prognoz 9* had similar time profiles and were coming from the same hemisphere in the sky, a fact that might indicate recurrence. The actual discovery of SGR 1806–20 was then the result of combining data from several spacecraft in the first and second interplanetary networks (Atteia et al. 1987; Laros et al. 1987; Kouveliotou et al. 1987). This third addition to the class was subsequently linked to an event in 1979.

The first detected burst from SGR 0526–66 was the famous 1979 March 5 event, unique in every observational aspect (Cline 1981), whose explanation still remains a challenge; it may be a link between SGRs and GRBs. It is the only event from an SGR source with a long-duration ( $> 2$  minute) decay portion: a well-defined (over 20 cycles) 8 s periodicity, strongly implying a neutron star origin. All other bursts from the three confirmed SGR sources have unique and rather uniform characteristics. Their durations are the shortest of all cosmic transients so far discovered, typically  $\sim 0.1$  s. Compared with “classical” gamma-ray bursts, SGR temporal profiles exhibit simple time histories, often with exponential decay or “flat-topped” profiles. The rise times are unresolved, with an upper limit of 5 ms for one burst (Kouveliotou et al. 1987). Their spectra have characteristic energies of  $\sim 30$  keV, with a distinct rollover below  $\sim 10$  keV. Relatively long bursts ( $\sim 250$  ms to  $\sim 1$  s or longer) from two SGRs show no spectral evolution on time scales as short as 128 ms (Golenetskii et al. 1984; Kouveliotou et al. 1987). The total numbers of events observed per source are 16, 3, and more than 100 bursts, with separations on time scales that vary stochastically from hours to years.

The direction to SGR 0526–66 has been measured with unprecedented accuracy in gamma-ray astronomy (Cline et al. 1982; Golenetskii et al. 1986). It is currently the smallest source field in gamma-ray astronomy, and lies superposed on the supernova remnant N49 in the Large Magellanic Cloud (LMC). SGR 1806–20 and SGR 1900+14 have much larger error boxes that lie very close to or overlap the Galactic plane. The centers of their respective source localization regions in

<sup>1</sup> Department of Physics, University of Athens.

<sup>2</sup> Postal address: ES-62, NASA/Marshall Space Flight Center, Huntsville, AL 35812.

<sup>3</sup> Universities Space Research Association (USRA).

<sup>4</sup> Code 668.1, Laboratory for High Energy Astrophysics, NASA/Goddard Space Flight Center, Greenbelt, MD 20771.

<sup>5</sup> Code 4121, E. O. Hulburt Center for Space Research, Naval Research Laboratory, Washington, DC 20375–5000.

<sup>6</sup> Code 661, Laboratory for High Energy Astrophysics, NASA/Goddard Space Flight Center, Greenbelt, MD 20771.

<sup>7</sup> Code 682, Laboratory for Astronomy and Solar Physics, NASA/Goddard Space Flight Center, Greenbelt, MD 20771.

Galactic coordinates are  $b = 9^{\circ}97$ ,  $l = -0^{\circ}24$  (Atteia et al. 1987) and  $b = 46^{\circ}6$ ,  $l = 4^{\circ}1$  (Mazets et al. 1979). If the N49 and Galactic disk source associations are accepted, all three sources lie in the direction of Population I regions, which may suggest an evolutionary link between SGRs and young objects (Kouveliotou et al. 1987). Several astronomical and energetics arguments discussed by Norris et al. (1991) support the hypothesis that SGR sources are located at distances of tens of kiloparsecs, in contrast to arguments that the N49 and Galactic disk source directions are accidental.

In this paper we consider observations of SGRs from the viewpoint of detection threshold criteria. Various instruments which have been capable of detecting SGR bursts afford differing sky coverage, collecting areas, burst-trigger integration times, and observational epochs. The Konus instruments on board *Venera 11-14* detected at least 15 bursts from SGR 0526-66 over a period of 5 yr (1978-1983), identified as sequels to the 1979 March 5 event. These were either too weak or too soft to be detected by other all-sky gamma-ray burst instruments. A limitation of the Konus detectors for detecting SGR bursts was the trigger integration time, of 0.2 s or longer, about twice as long as the usual SGR durations. Like HXRBS on *SMM*, the *ICE* instrument did not require a trigger to record a burst; using real-time data with 0.5 s resolution, it detected over 110 bursts from SGR 1806-20 from 1979 through 1984 (Laros et al. 1987). Twelve of these events in 1983 were also detected by the *Prognoz 9* Soviet satellite (Atteia et al. 1987). Since 1985, transmission of data from *ICE* became increasingly limited until it stopped in 1987. The *Prognoz 9* spacecraft ceased operation in 1984.

*SMM* was for nearly a decade, from its launch in 1980 until its demise in late 1989, one of the few satellites with an instrument sensitive to the spectral region in which SGRs emit the bulk of their radiation. Furthermore, over this period HXRBS was the only instrument operating on very short trigger integration times of 4, 32, and 256 ms, which best suited an organized search for any recording of SGR-type transients. For this search the time resolution was set to 1 ms. Observations of SGR 1806-20 with HXRBS on *SMM* (Kouveliotou et al. 1987) include evidence for a possibly distinct component of low-level emission, for rapid rise and decay times ( $\leq 5$  ms), and for a lack of spectral variability on a 0.1 s time scale. Similarly, in two flat-topped bursts from SGR 0526-66, Konus detected no spectral variability on a 0.5 s time scale (Golenetskii et al. 1984).

Nearly continuous coverage with 64 and 128 ms time resolution data has been provided by *SMM*, except for 8 months prior to the time of the repair mission in 1984 April. A search through these high time resolution data provides both a 4 yr extension beyond 1985 of *ICE*'s coverage of SGR 1806-20, when it is found in the  $40^{\circ}$  (FWHM) field of view during December and January of each year, and a survey for bursts from other SGR sources within  $40^{\circ}$  of the Sun. Over the whole year of 1987, the instrument was appropriately reconfigured, by command from the ground, to obtain the best time resolution and sensitivity available. The HXRBS low-energy threshold ( $\sim 30$  keV) and its sensitivity to SGR bursts in this optimum configuration are superior to the *ICE* instrument beyond 1984 (Laros et al. 1987) and similar to those of the Konus instruments (Mazets & Golenetskii 1981), with the exception that HXRBS had a smaller field of view. In addition, HXRBS had an active anticoincidence shield.

We have collected and analyzed memory data for a total of

about 4000 burst triggers, out of which only a very few could be considered as valid SGR candidate events. In the next section we outline the search methodology, calculate the HXRBS exposure and sensitivity to SGR bursts, describe criteria which constrain the number of candidate events, present the statistics of our results, and give an upper limit for the SGR source number density. In the discussion section (§ 3) we apply this limit, combined with results from other relevant observations and the assumption of a neutron star origin, to obtain a constraint on SGR-active lifetimes. Source distributions, probable energy release processes, and viable emission mechanisms are discussed in a previous paper (Norris et al. 1991).

## 2. SEARCH METHODOLOGY AND RESULTS

### 2.1. Instrumentation

The HXRBS detector (Orwig, Frost, & Dennis 1980) is a CsI(Na) scintillator (area  $68 \text{ cm}^2$ , thickness 0.64 cm), actively shielded by a cylindrical well-type CsI(Na) crystal with a wall thickness of 3.2 cm. From launch until 1980 December and from 1984 April to the end of operation in 1989 October, the instrument axis has generally been pointed to within  $0^{\circ}.5$  of the Sun center, except for occasional off-points to view nonsolar sources. During the greater than 3 yr interval after the failure of the *SMM* fine-pointing system in 1980 December, the axis precessed about the direction to the Sun with a coning angle as large as  $15^{\circ}$ . Central crystal events in anticoincidence with the shield are pulse-height-analyzed to produce 15 channel energy-loss spectra every 128 ms over the energy range from  $\sim 30$  to 500 keV. A burst trigger is generated if the number of these events from the central detector exceeds a preset value in one or more of three fixed (4, 32, and 256 ms) time intervals. Counts (but no spectral or live-time information) are stored in a circulating memory with a time resolution that was set at 10, 5, and 1 ms at different times during the mission. The memory has a capacity of recording these data in 32,768 consecutive time intervals, with two-fifths of the samples recorded immediately before the trigger and three-fifths after. The contents of the memory are read out at a later time. The shield crystal also serves as a collimator giving HXRBS a circular field of view with an approximately triangular geometric response function with a FWHM of  $\sim 40^{\circ}$ , a cutoff at  $44^{\circ}$  off-axis, and a solid angle of 1.5 sr. The relatively soft SGR bursts are not detectable through the shield.

### 2.2. Search Methodology

In order to optimize our chances for detecting SGRs and to allow us to set limits on the rate of SGRs, we developed the following search pattern using both archival (i.e., non-interactive) and near-real-time studies.

We performed an archival data search for all the years since launch for one month centered on December 23 of each year of the mission. During this period, the most active SGR known, 1806-20, is within  $30^{\circ}$  of the HXRBS axis, i.e., well within the field of view. During much of the mission, timing data from other spacecraft could be used, in principle, to confirm and to constrain the source positions of candidate events. The search however, was constrained by the system configuration, where time resolution, and energy and trigger thresholds, were each occasionally varied. Another limitation was due to the partial activation for preservation purposes, in late 1983, of the *SMM* tape recorders for the Shuttle repair mission, performed in 1984 April. This time period, unfortunately, was exactly when

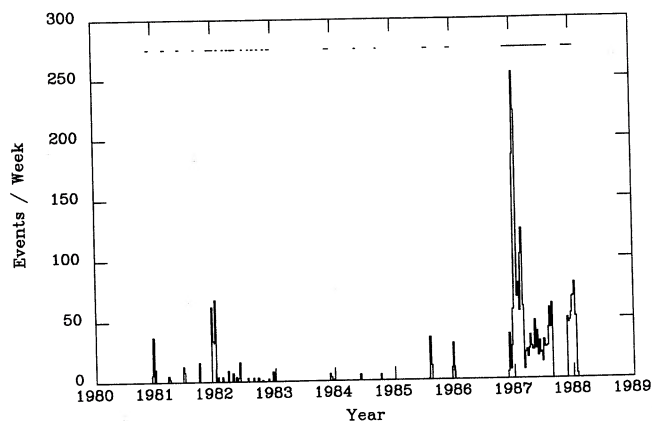


FIG. 1.—Number of events per week detected in the HXRBS central crystal and recorded by the triggered high time resolution memory. Search concentrated on triggers during the period 1986 November–1988 January and during periods of passage of the Galactic center through the instrument field of view.

SGR 1806–20 exhibited exceptional burst activity (Laros et al. 1987); most of the bursts that HXRBS might have detected were therefore not recorded.

In 1986 November, after the discovery of SGR 1806–20, we initiated an “SGR-optimized” search mode. Our main objectives were both to extend coverage of SGR 1806–20 after *ICE* had effectively ceased transmission of data and to look for additional new sources. Since this search was done in near-real time, we could now interactively determine the parameters for an optimal instrument configuration for detection of SGR-like bursts. We set the highest time resolution available (1 ms), and we experimented with different gains and trigger thresholds to maximize sensitivity to SGR bursts while avoiding an excessive number of triggers from energetic particles. In this mode we have collected and examined all the memory triggers for a 10 month period starting in 1986 December and ending in 1988 January, with a two-month gap in 1987 August and September.

The resulting total time coverage of the search is shown schematically in Figure 1 by the solid lines extending along the upper part of the figure. In the lower part is plotted the number of triggers per week recorded during the searched periods over 9 yr. The peak centered at the beginning of 1987 is due to a higher gain setting during this period, which resulted in a threefold increase of the trigger rate. Other fluctuations in the rate reflect experimentation with the configuration settings, rather than true data changes. The lack of triggers around 1983 December–1984 January is artificial, as explained in the previous paragraph. In fact, we have completely covered both months searching for triggers, but the very limited duty cycle of 10 minutes per orbit of HXRBS before its Shuttle repair barely included any trigger dumps. For the same part of the year in 1985–1986 we decided not to search, after discovering a faulty dump command which made 90% of the dumps useless. All the various “on” times were combined to calculate the total exposure and sensitivity of HXRBS to SGR emissions.

### 2.3. Calculation of the Exposure to SGR Emissions

The “dead” times involved during the intervals covered by our search are the satellite nights, the passages through the South Atlantic Anomaly (SAA), and the 3 minute duration of

daytime memory dumps. The following three memory-dump modes were used at different times during the mission:

1. The normal dump mode was the default and most frequently used configuration, designed to allow for the uninterrupted recording of solar flare data. In this mode, if a trigger occurs during the daytime part of the *SMM* orbit, the memory fills and it is read out at the beginning of satellite night.

2. The trigger and dump mode was used exclusively to study SGR 1806–20 during the period when it was within the FWHM field of view of HXRBS, from mid-December to mid-January in 1986/1987 and in 1987/1988. The data are written to the on-board tape recorder immediately after the memory is filled, and the memory trigger is then immediately reactivated, thus allowing for the maximum possible time per orbit when the instrument could record a burst in the memory. The exposure calculated during this period gives an upper limit on the activity of SGR 1806–20.

3. The intermediate mode, in which the memory was permitted to trigger twice but dump only once in the daytime part of the orbit, was used for short periods, usually (but not necessarily) following the trigger and dump mode. In this way we kept the number of triggers higher than usual so as to record any fortuitous SGR 1806–20 bursts as it left our field of view, without compromising the collection of solar flare data. This procedure results in only one 3 minute gap during the day, since the next trigger is dumped immediately after the beginning of spacecraft night.

The calculation of the exposure of HXRBS to SGR bursts is broken into the following time intervals according to the different operating modes:

1. 1986 November–1988 January (normal and intermediate mode).—We calculate and add the daytime part of the orbits up to the first trigger times. In the rest of the orbit the memory is full and not sensitive to another burst. A variation of this method is applied for the intermediate mode, where we have up to two triggers per satellite day. The exposure thus calculated is  $1.69 \times 10^7$  s. The ratio of this live time to the total daytime in this mode gives a duty cycle of 46%.

2. 1980–1986 (all intervals) and 1988 (normal and intermediate mode).—For these two intervals we assumed the same value of duty cycle as above and computed the exposure times of  $6.20 \times 10^6$  s and  $0.41 \times 10^6$  s, respectively.

3. 1986 December 20–1987 January 30 and 1987 December 23–1988 January 5 (trigger and dump mode).—Here the exposure time includes all the daytime part of each orbit except for the 3 minute memory dumps and SAA passages. The total exposure time for these two intervals was determined to be  $2.75 \times 10^6$  s.

The resulting total exposure time from 1980 to 1988 is  $2.62 \times 10^7$  s, or 0.83 yr. Thus, on average our search is equivalent to a 100% exposure for random SGR-like emissions, for a 10 month period in which any given source along the ecliptic plane has roughly a 10% duty cycle. After 1986 November for almost 1 year we operated on a 46% duty cycle. In particular, for SGR 1806–20, during the 54 days in which we activated the trigger and dump mode, we obtained a 60% duty cycle.

### 2.4. Sensitivity Calculation

The HXRBS memory has three trigger circuits which sum counts every 4, 32, and 256 ms and compare the totals with

commandable trigger values. Since the false trigger rate is dominated by energetic particle events lasting less than  $\sim 30$  ms, the 4 ms and 32 ms trigger thresholds were effectively disabled for  $\sim 30\%$  of the time (i.e., set equal to a high threshold), and the remaining 256 ms count threshold was then varied between 40 and 260 counts in combination with the detector's gain state. In 1987 the nominal gain state set for HXRBS corresponds to an energy range of 34–566 keV. During the SGR 1806–20 search in 1987, we experimented with the gain setting in order to optimize sensitivity by limiting the number of memory triggers per orbit; one higher gain state (20–303 keV) was used for a short period, which resulted in tripling the average number of triggers per orbit. The average sensitivity to SGR bursts over all searched data intervals is then calculated as follows:

The average fraction,  $f_{\text{area}}$ , of the central crystal area ( $A = 68 \text{ cm}^2$ ) exposed to a source within  $30^\circ$  of the instrument axis, i.e., within the full-width quarter-maximum (FWQM) field of view, is 0.5 (Norris 1983). If we assume an SGR-like input photon spectrum with  $\langle E \rangle = 1.44E_{\text{low}}$ , where  $\langle E \rangle$  is the average photon energy in keV, and  $E_{\text{low}} = 30 \text{ keV}$  is the lower energy threshold, the sensitivity,  $F$ , is given by

$$F \sim (1.6 \times 10^{-9} C \langle E \rangle) / (f_{\text{area}} A) \text{ ergs cm}^{-2}, \quad (1)$$

where  $C$  is the number of counts required to trigger the memory.

Thus, during the two modes which were not “trigger and dump,” where the average value of  $C$  was 200, the sensitivity was about  $4 \times 10^{-7} \text{ ergs cm}^{-2}$ . In the oriented search for bursts from SGR 1806–20, in the trigger and dump mode, the highest sensitivity achieved (with a setting of  $C = 40$ ) was about  $8 \times 10^{-8} \text{ ergs cm}^{-2}$ , during 1986 December–1987 January.

In both cases the solid-angle coverage within the FWQM field of view was  $0.84 \text{ sr} = 0.067 \times \text{full sky}$ . SGR bursts lasting  $\sim 30$  ms could have been detected from the Galactic center region at flux levels of  $\sim 3 \times 10^{-6} \text{ ergs cm}^{-2} \text{ s}^{-1}$ . This flux is one order of magnitude lower than the fluxes of the brighter bursts observed from SGR 1806–20 (Atteia et al. 1987) and is

comparable to the fluxes observed in bursts detected with Konus from SGR 0526–66 (peak fluxes  $\sim 2.6 \times 10^{-6} \text{ ergs cm}^{-2} \text{ s}^{-1}$ ) (Golenetskii et al. 1986). We note that if the latter burster were indeed located in the LMC (see, e.g., Norris et al. 1991), the HXRBS sensitivity would have been sufficient to detect SGR-like bursts from the entire Galaxy.

### 2.5. Statistics and Nature of Spike Events

Statistical analysis of the approximately 4000 events collected over the total search period covers memory triggers recorded during satellite night, as well as the day part of the orbit, mainly for comparison purposes. Figures 2a and 2b show histograms of the event frequency distribution versus its full-width zero-amplitude (FWZA) duration, for day and for night events, respectively. The circles, triangles, and squares correspond to different trigger accumulation intervals and are summed up to give the total distribution (*solid line*), which appears to be similar for day and night events. The plots are limited at short durations by the 1 ms minimum time resolution of HXRBS. Although part of the events were recorded with time resolutions of 5 and 10 ms, the majority were recorded with 1 ms resolution. There appear to be two minima in the distributions, one between 2 and 3 ms and one between 6 and 10 ms, that cannot be explained by uncertainties in the duration measurements. An extensive study of the detailed experiment configuration conditions, during which these minima are present, showed that the first appears only at small (40) integration count numbers, while the second is almost always present in the distributions. The overall picture suggests that the events can be divided into three duration regimes:

1. *Very short events* (FWZA  $< 2$  ms).— These are less intense events, and they have been recorded only when the trigger threshold requirements were set to 40 counts over 256 ms. They have a very soft spectrum.

2. *Short events* (FWZA between 3 and  $\sim 6$  ms). These events are structureless with a simple rise and decay, with soft spectra extending in energy to less than 70 keV. We believe that they

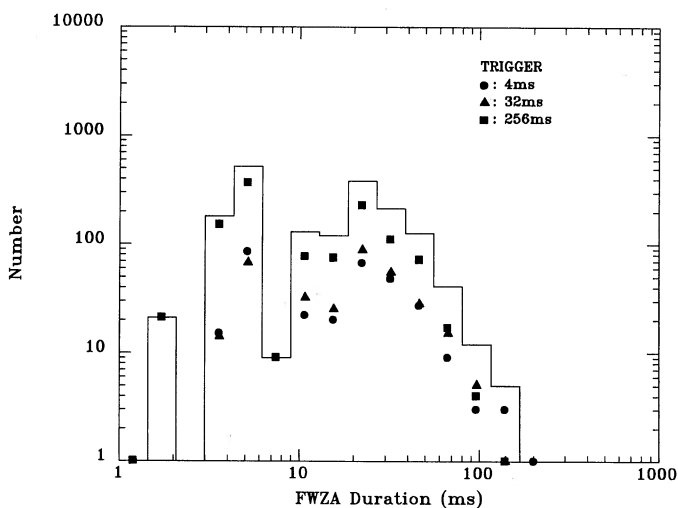


FIG. 2a

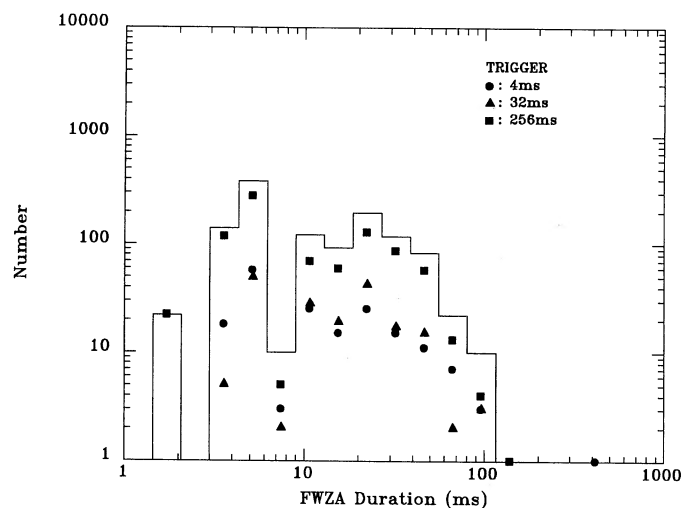


FIG. 2b

FIG. 2.—Event frequency distribution vs. duration. (a) Satellite day events; (b) satellite night events. Squares, circles, and triangles correspond to different trigger accumulation times and are summed to give the total distribution (*solid line*). The plots include all triggers recorded with varying instrument configurations, such as different gains, trigger thresholds, and time resolutions.

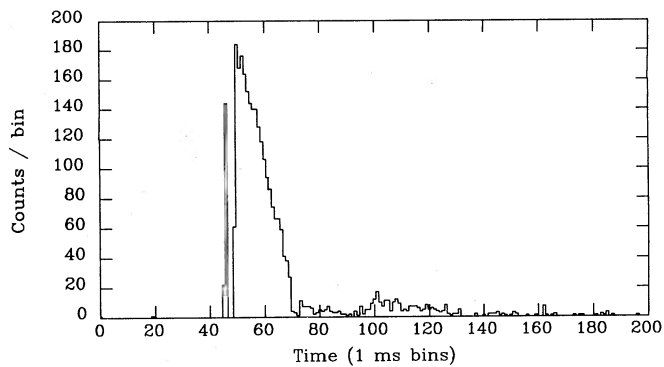


FIG. 3a

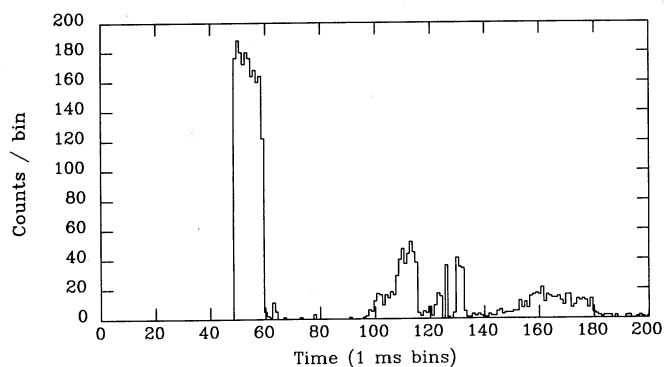


FIG. 3b

FIG. 3.—Time profiles of two “noise” events recorded with 1 ms time resolution. (a) A typical intense short event with a steep rise and a structureless decay. (b) An exceptionally structure-rich event, exhibiting an initial intense rise followed by a low-intensity tail of duration  $\sim 100$  ms. The gap occurring directly after event onset is discussed in the text.

manifest a very quick recovery from saturation of the electronics of the system, probably due to large energy deposition by low-Z cosmic rays on the central crystal. They comprise about 30% of the total events.

3. *Longer events* (duration FWHM  $\sim 20$  ms; FWZA between  $\sim 10$  and 120 ms).—The bulk of these can be described as showing a very steep rise followed by an exponential decay that may last up to 100 ms. Their energy spectra are fitted either with an exponential thermal bremsstrahlung with  $kT = 20$  keV or, in some cases—within the available 5 channel statistics—equally well with a power law with spectral index of about  $-4.5$ . In these events the maximum energy never exceeded 150 keV, the average being about 100 keV.

Figure 3 illustrates two intense “noise” events recorded with 1 ms time resolution; Figure 3a shows an event with the typical steep rise and structureless decay, followed by a low-intensity tail (the dip to background level, 2 ms after event onset, is due to an instrumental artifact, discussed below). Figure 3b shows an example of an event with exceptionally rich structure. Approximately 40 events of this type were identified in HXRBS data with a characteristic signature that includes an initial intense spike, about one order of magnitude more intense than the brightest SGR bursts, followed by a low-intensity tail of duration 50–150 ms. A typical feature of these events, not observed in SGR bursts, is the (nearly) complete absence of counts during some portions of the tail; often the appearance suggests oscillatory behavior. None of these events with tails

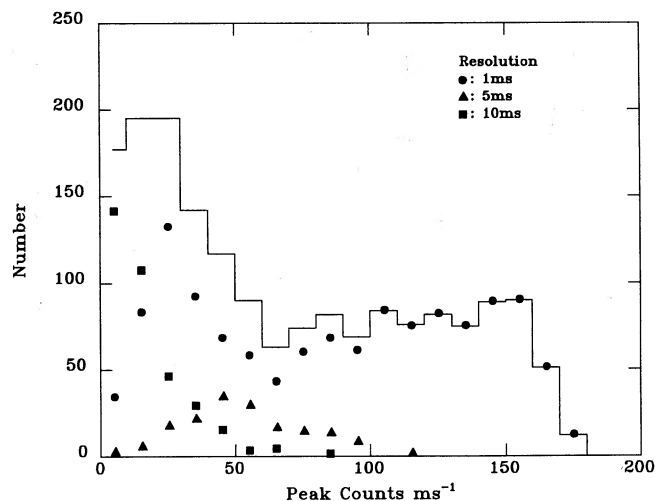


FIG. 4.—Histogram of the number of events vs. peak count rate. Squares, circles, and triangles correspond to the different time resolutions (1, 5, and 10 ms) with which the events were recorded.

has been confirmed with the X-ray detectors of *SMM*'s gamma-ray spectrometer (D. Messina 1989, private communication) or with the Los Alamos X-ray detector on *Pioneer Venus Orbiter (PVO)* (R. Klebesadel 1989, private communication) or with the gamma-ray spectrometer on the Mir Space Station (R. Sunyaev 1989, private communication).

Figure 4 shows the number of events versus peak count rate. The events recorded with 1 ms resolution (the statistically largest sample with the best resolution) show a flat distribution averaging about 80 events at most intensities. The significant deviation of the distribution of the other time resolutions (5 and 10 ms) from a flat profile is indicative of the strong dependence on the electronics configuration. It adds to the argument that these events are mainly due to triggers from fluctuations about the mean value of the phosphorescent pulse (Hurley 1978): longer integration times (10 ms) tend to smooth out and reduce the number of the fluctuations (recorded as individual counts by the system's electronics), hence the shift of the bulk of the events toward the smaller peak intensities.

We conclude that the complex structure of these events, as well as the two peaks in the distribution of Figures 2a and 2b, are most probably characteristic of the particular detector and its electronics configuration. The peaks could be directly related to the passage of a high-Z cosmic-ray particle or many particles resulting from a cosmic-ray interaction in the detector or surrounding material. The anticoincidence counter is designed to reject such charged particle events, but it may also become saturated and may not fully recover prior to the end of the veto pulse.

Similar events, previously observed by other investigators with balloon-borne detectors, are generally attributed to the long-lived ( $\sim 150$  ms) phosphorescent component of the NaI(Tl) crystal (Johnson, Kurfess, & Bleach 1975; Fishman & Austin 1976; Hurley 1978). Emigh & Megill (1954) showed that this component decays in a monomolecular process with a mixture of exponential components. Koicki, Koicki, & Ajdacic (1973) demonstrated that the fractional contribution of this process is at least 10% of the light emitted from the crystal, and that its intensity is linear with the absorbed radiation energy, at least up to 1 MeV.

The source of these events is believed to be very large energy depositions in the crystal. Johnson et al. (1975) have reproduced similar pulse profiles by irradiating NaI(Tl) and CsI(Na) crystals with very high energy gamma-rays ( $>10^4$  GeV). Hurley (1978) compares the expected rates of these spiky events for balloon-borne experiments with the observed ones for two different particle populations (protons and Fe group nuclei) and two physical procedures (ionization losses and nuclear reactions inside the crystal). He concludes that, for balloon altitudes, the rates observed can be attributed to nuclear interactions of heavy nuclei (Fe group) in a CsI(Na) or CsI(Tl) crystal, with energy losses up to  $60 \text{ GeV g}^{-1} \text{ cm}^{-2}$ .

The *SMM* event rate for Fe group nuclei, based on nuclear interactions in the crystal and taking into account the zero residual atmosphere of the spacecraft, is  $5 \times 10^{-6} \text{ events s}^{-1}$ . This is two orders of magnitude lower than the total event rate actually observed by the HXRBS, which is  $1.5 \times 10^{-4} \text{ events s}^{-1}$ . The most likely explanation for this higher rate is the limitation of the HXRBS anticoincidence pulse, which had a maximum duration of the order of 1 ms: many of the events studied here persist for durations one to two orders of magnitude longer than the anticoincidence mask. Because of this limitation, we believe that energy deposited in the central crystal necessary to produce enough false pulses to trigger the memory (although not actually known) could be considerably lower than that deposited by an Fe group nucleus. Thus lighter nuclei can also cause a memory trigger, significantly contributing to the observed rate. Also, one has to take into account the statistics of high fluctuations in longer (than balloon experiments) data sets. Considering all the above, we conclude that the rate observed from the HXRBS is not inconsistent with the balloon results reported previously and reflects the noise environment of a CsI(Na) crystal on board a spacecraft.

The general consensus of this work and previous results is that events resulting from the deposition of large amounts of energy from charged particle interactions in the scintillation crystal should be simple in structure, with sharp rise and exponential decay. The only other possible feature, mentioned by Johnson et al. (1975) and Fishman & Austin (1976), is a sudden dip in the count rate immediately after the onset of the event, which is attributed to space-charge effects and charge depletion on dynode coupling capacitors. The same effect is apparent in our data in most events with 1 ms resolution and in some of the events with lower time resolutions (see Figs. 3a and 5d), and is also reflected in the 2–3 ms gap in the distribution of durations.

### 2.6. Candidate Events

We have used several techniques to expedite our search for candidate SGR events among the large number of memory triggers. The following restrictions were placed on the memory dumps that were examined in detail:

1. Events with a strong shield response were excluded. Many of the triggers were accompanied by a shield signal indicating off-axis sources and/or charged cosmic-ray particles.
2. Events with a coincident response in the HXRBS particle detector were excluded.
3. Events with spectra unlike a soft SGR-like spectrum were excluded.

Of the 4000 triggers, approximately 40 interesting events remained after applying these rejection criteria. Most of these had a signature that included an initial intense spike, about

one order of magnitude more intense than the brightest SGR bursts, followed by a low-intensity tail lasting for up to 150 ms. A typical feature of nearly all these events, which has not been observed in SGR bursts, is the total absence of counts during some portion(s) of the time history (in addition to the dip immediately following event onset, described in the previous section); in fact, the time profile often has an oscillatory appearance. Events exhibiting a long hiatus were also discounted, since these gaps are believed to be due to saturation of electronics. Furthermore, none of these extended events were confirmed with the X-ray detectors of *SMM*'s gamma-ray spectrometer (D. Messina 1989, private communication) or with the Los Alamos GRB detector on *ICE* (J. Laros 1989, private communication) or with the Los Alamos GRB detector on *PVO* (R. Klebesadel 1989, private communication) or with the gamma-ray spectrometer on the Mir Space Station (R. Sunyaev 1989, private communication).

After combining the above restrictions, and demanding SGR-like appearance and a daytime trigger, only five residual candidate events remained. These events all have profiles and spectra that in various respects resemble those of SGRs, including an initial sharp rise ( $<5$  ms), a flat peak with a duration ranging from 25 to 45 ms, and a steep decay ( $<10$  ms) as shown in Figure 5. One is a confirmed SGR burst (Fig. 5a), described in Kouveliotou et al. (1987). The other four candidate events are all consistent with a thermal bremsstrahlung fit with  $kT \sim 20$  keV.

For one of the events (Fig. 5d), observed in 1987 February, the GRB monitor on *PVO* detected a  $3.7 \sigma$  single increase of duration less than 0.5 s, within the possible time window of about 1000 s (R. Klebesadel 1989, private communication). A location using the *SMM* and *PVO* arrival times give a source locus consisting of a ring, which is entirely within the hemisphere around the Galactic anticenter. No other instrument has seen any increase consistent with any of the remaining three candidate events. We thus conclude that, during the 0.83 yr of our time coverage with HXRBS, there were five bursts at most that could be attributed to an SGR-type source.

### 3. DISCUSSION

Our survey of HXRBS data has provided an additional SGR monitor. The product of the FWHM field of view (0.38 sr) and the total instrument observing period (0.83 yr) is  $0.32 \text{ sr yr}$ , significantly less than the  $\sim 4 \text{ sr yr}$  exposure obtained by *ICE* during its lifetime. The HXRBS total exposure is  $\sim 7\%$  of that from each of the Konus instruments on *Venera 11–14*. These values represent isotropic coverage for the *Venera* satellites, but directional coverage confined to regions near the ecliptic plane for *ICE* and HXRBS. With its  $10^\circ$  wide band *ICE* had a 100% duty cycle on the plane, whereas with its  $80^\circ$  wide field of view HXRBS had roughly a 10% average duty cycle for any given point on the plane. Thus, for a given source near the ecliptic, such as SGR 1806–20, HXRBS obtained about 30 days of exposure. We note that the major fractions of HXRBS and *ICE* coverage are not in the Galactic plane. Therefore, the tendency would have been preferentially to detect sources out of the plane if the parent population were isotropically distributed.

The enhanced HXRBS sensitivity during the study of the Galactic center region was  $8 \times 10^{-8} \text{ ergs cm}^{-2}$ . This means that a non-Earth-occulted event within  $30^\circ$  of the center of the field of view would have been detected even if it were one order of magnitude weaker than any of the confirmed events

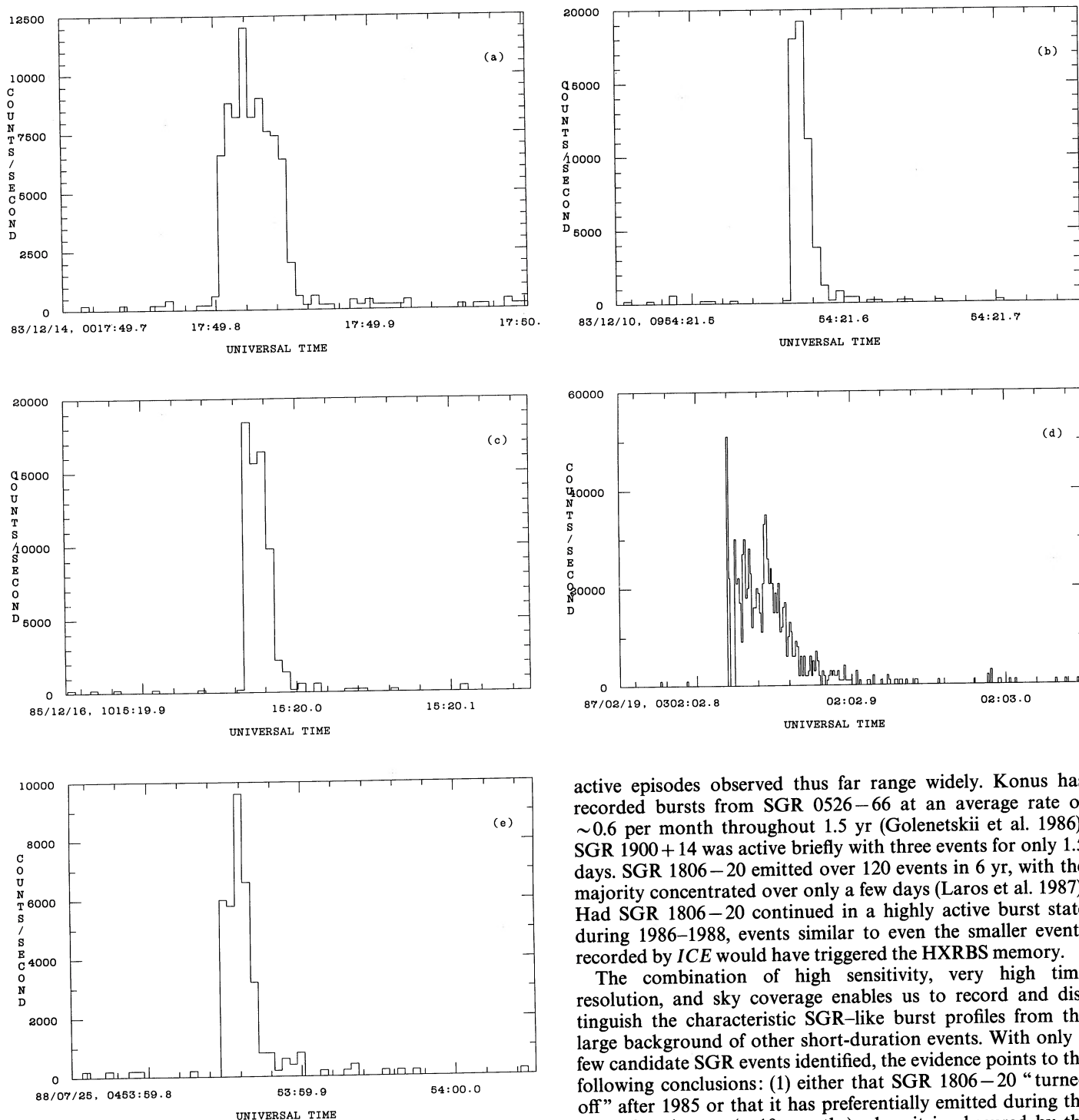


FIG. 5.—Time profiles of five events detected with HXRBS in the circulating memory. (a) A confirmed event from SGR 1806–20 recorded with 5 ms time resolution (see Kouveliotou et al. 1987). (b–d) Potential SGR burst candidates discovered during the archival data search. Time resolution is 5 ms for (b), (c), and (e), and 1 ms for (d).

observed by *Prognos 9* from SGR 1806–20 (Atteia et al. 1987). For the rest of the sky coverage, the typical or unenhanced HXRBS sensitivity was  $4 \times 10^{-7}$  ergs  $\text{cm}^{-2}$ .

The three known SGR sources provide a very tenuous picture of what to expect in terms of lifetime activity. The

active episodes observed thus far range widely. Konus has recorded bursts from SGR 0526–66 at an average rate of  $\sim 0.6$  per month throughout 1.5 yr (Golenetskii et al. 1986). SGR 1900+14 was active briefly with three events for only 1.5 days. SGR 1806–20 emitted over 120 events in 6 yr, with the majority concentrated over only a few days (Laros et al. 1987). Had SGR 1806–20 continued in a highly active burst state during 1986–1988, events similar to even the smaller events recorded by *ICE* would have triggered the HXRBS memory.

The combination of high sensitivity, very high time resolution, and sky coverage enables us to record and distinguish the characteristic SGR-like burst profiles from the large background of other short-duration events. With only a few candidate SGR events identified, the evidence points to the following conclusions: (1) either that SGR 1806–20 “turned off” after 1985 or that it has preferentially emitted during the part of each year ( $\sim 10$  months) when it is obscured by the HXRBS shield and (2) that no other SGR source was highly active during the same period near the Galactic center (within the HXRBS field of view). We further note that during 1980–1983 (when HXRBS was scanning in the typical, nonenhanced mode) it serendipitously detected four bursts from SGR 1806–20 (Kouveliotou et al. 1987). *Continuous* burst activity from this source or from any Galactic source within  $\sim 30^\circ$  of the ecliptic plane should, therefore, have been detected with HXRBS. SGR 0526–66 is near the south ecliptic pole and therefore could not be studied with HXRBS.

Thus, the evidence suggests either that the total active lifetimes of the SGR sources may be short or that their number may be very small. This result is consistent with the previous result that, in its cumulative 3.2 yr all-sky exposure, Konus detected events from only three confirmed SGR sources. We follow the line of reasoning of Kouveliotou et al. (1989) and Norris et al. (1991). We may constrain the SGR-active lifetime in terms of the fraction of neutron stars which become SGRs from these considerations, if we make the assumption that SGRs must be neutron stars. Furthermore, assuming a supernova origin for these neutron stars (and steady state source populations), the number of active SGRs at any given time is given by

$$N_{\text{SGR}} = R_{\text{ns}} \tau_{\text{ns}} f_{\text{SGR}}(\tau_{\text{SGR}}/\tau_{\text{ns}}), \quad (2)$$

where  $R_{\text{ns}}$  is the neutron star production rate (i.e., the supernova explosion rate),  $\tau_{\text{ns}}$  is the neutron star lifetime in the Galaxy, and  $f_{\text{SGR}}$  is the fraction of neutron stars that become SGR sources. Solving for the SGR-active lifetime yields

$$\tau_{\text{SGR}} = N_{\text{SGR}}/(R_{\text{ns}} f_{\text{SGR}}). \quad (3)$$

The inclusive duration of SGR activity for a source is not well constrained, but  $\tau_{\text{SGR}}$  is a meaningful quantity: it is the sum of all SGR-active periods during a source's lifetime. Since  $N_{\text{SGR}}$  and  $R_{\text{ns}}$  are fairly well constrained,  $\tau_{\text{SGR}}$  is, to first order, dependent on the estimate of the fraction of neutron stars which become SGRs. An estimate is obtained if we assume that all neutron stars pass through an SGR state, i.e.,  $f_{\text{SGR}} = 1$ . In that case, using a very rough estimate for  $N_{\text{SGR}}$  of 10 (greater than the 3 observed; see discussion on duration of "SGR-active" periods in Norris et al. 1991) and the observed supernova rate of 1 per 50 yr, we obtain

$$\tau_{\text{SGR}} \sim 500 \text{ yr}. \quad (4)$$

The value of  $f_{\text{SGR}}$  is dependent on the assumed parent population. An independent argument by Norris et al. (1991) yields a similar value for  $\tau_{\text{SGR}}$ , assuming that SGRs are an evolutionary stage following radio pulsars. However, if the SGR-active state were to occur only during the radio pulsar lifetime, then the estimate of  $\tau_{\text{SGR}}$  increases, e.g., by the ratio of neutron star lifetime ( $\sim 10^{10}$  yr) to pulsar lifetime ( $\sim 10^7$  yr). Thus, either  $f_{\text{SGR}}$  is extremely small, e.g., SGRs are quiet rare sources, and/or  $N_{\text{SGR}}$  is very large, but the duty cycle of each source is extremely low so that only a few SGR emissions could be detected during a satellite's lifetime.

Future observations, especially with the Burst and Transient Source Experiment (BATSE) on board the *Compton Gamma-Ray Observatory*, will extend the monitoring of SGRs to  $\sim 16$  yr. BATSE is a sensitive all-sky monitor which affords more than an order of magnitude improvement in sensitivity over the previous generation of GRB experiments. It has microsecond timing with spectral coverage down to  $\sim 15$  keV, and capability for localization down to arcminute scales, for brighter bursts (Fishman et al. 1989). With any fortuitous detection, BATSE could contribute to the determination of the SGR source distribution (on or outside the Galactic plane) and lead to the clarification of the SGR source nature and statistics.

We wish to thank K. Hurley and J. G. Laros for helpful discussions. The technical assistance and endurance of K. Tolbert, S. Kennard, D. Biesecker, and T. K. Koshut contributed significantly to the laborious task of searching the thousands of HXRBS trigger dumps. This work was supported by the Office of Naval Research and the National Aeronautics and Space Administration.

#### REFERENCES

- Atteia, J.-L., et al. 1987, *ApJ*, 320, L105  
 Cline, T. L. 1981, *Ann. NY Acad. Sci.*, 375, L45  
 Cline, T. L., et al. 1982, *ApJ*, 255, L45  
 Emigh, C. R., & Megill, L. R. 1954, *Phys. Rev.*, 93, 1190  
 Fishman, G. J., & Austin, R. W. 1976, *Nucl. Instr. Meth.*, 140, 193  
 Fishman, G. J., et al. 1989, *Proc. Gamma Ray Observatory Science Workshop*, ed. W. N. Johnson (Greenbelt: NASA/GSFC), 2-39  
 Golenetskii, S. V., Aptekar, R. L., Gur'yan, Yu. A., Il'inskii, V. N., & Mazets, E. P. 1986, *IOFFE Physics & Technology Institute*, preprint  
 Golenetskii, S. V., Il'inskii, V. N., & Mazets, E. P. 1984, *Nature*, 307, 41  
 Hurley, K. 1978, *A&A*, 69, 313  
 ———. 1986, talk presented at Conf. on Gamma-Ray Stars (Taos, NM)  
 Johnson, W. N., Kurfess, J. D., & Bleach, R. D. 1975, talk presented at COSPAR Symposium (Varna, Bulgaria)  
 Koicki, S., Koicki, A., & Ajdacic, V. 1973, *Nucl. Instr. Meth.*, 108 (No. 2), 297  
 Kouveliotou, C., et al. 1987, *ApJ*, 322, L21  
 Kouveliotou, C., Norris, J. P., Wood, K. S., Cline, T. L., Desai, U. D., Dennis, B. R., & Orwig, L. E. 1989, in *Proc. GRO Science Workshop*, ed. W. N. Johnson (Greenbelt: NASA/GSFC), 4-497  
 Laros, J. G., et al. 1987, *ApJ*, 320, L111  
 Mazets, E. P., & Golenetskii, S. V. 1981, *Ap&SS*, 75, 47  
 Mazets, E. P., Golenetskii, S. V., & Gur'yan, Yu. A. 1979, *Soviet Astron. Lett.*, Vol. 5 (No. 6), 343  
 Norris, J. P. 1983, Ph.D. thesis, Univ. Maryland (NASA TM-85031)  
 Norris, J. P., Hertz, P., Wood, K. S., & Kouveliotou, C. 1991, *ApJ*, 366, 240  
 Orwig, L. E., Frost, K. J., & Dennis, B. R. 1980, *Sol. Phys.*, 65, 25